

Original article

3D-QSAR study of sulfonamide inhibitors of human carbonic anhydrase II

Huoqiang Huang^{a,b}, Xulin Pan^{a,b}, Ninghua Tan^{a,*}, Guangzhi Zeng^{a,b}, Changjiu Ji^{a,b}^a State Key Laboratory of Phytochemistry and Plant Resources in West China, Kunming Institute of Botany, Chinese Academy of Sciences, Kunming, Yunnan 650204, China^b Graduate School of the Chinese Academy of Sciences, Beijing 100039, China

Received 12 June 2006; received in revised form 21 July 2006; accepted 21 September 2006

Available online 21 November 2006

Abstract

3D-QSAR models of Comparative of Molecular Field Analysis (CoMFA) and Comparative of Molecular Similarity Indices Analysis (CoMSIA) of 61 potent carbonic anhydrase II (CAII) sulfonamide inhibitors were performed using two methods. The conventional ligand-based 3D-QSAR studies were performed based on the lower energy conformations employing database alignment rule. The receptor-based 3D-QSAR models were also derived using bioactive conformations obtained by docking compounds to the active sites of CAII. The receptor-based model gave q^2 values of 0.623 and 0.562, r^2 values of 0.986 and 0.987 for CoMFA and CoMSIA, respectively, which were much better than those of ligand-based model (q^2 values of 0.532 and 0.466). The predictive ability of the models was validated using the test set of 10 compounds that were not included in the training set of 51 compounds. Results of CoMFA and CoMSIA suggested that heterocyclic sulfonamides are more active than aromatic sulfonamides, in the latter 1,3,5-triazole group substituting one hydrogen atom of the amido is favored and moderate groups in its 4- and 6-position are required. These results provided further understanding of the relationship between the structural features of CAII and its activities, which should be applicable to design and find new potential CAII inhibitors.

© 2006 Elsevier Masson SAS. All rights reserved.

Keywords: Carbonic anhydrase II; 3D-QSAR; Sulfonamide

1. Introduction

Carbonic anhydrases (CAs) are a family of zinc metallo enzymes, which catalyses the reversible hydration of CO₂ and water: $\text{CO}_2 + \text{H}_2\text{O} \leftrightarrow \text{H}^+ + \text{HCO}_3^-$. Five types of CAs including α -, β -, γ -, δ - and ϵ -CA are ubiquitously found in almost all kinds of organisms except fungi. All known CAs from higher vertebrates are of α -type, in which seven isoenzymes are found in human being including carbonic anhydrase II (CAII; E.C. 4.2.1.1) [1,2].

hCAII, the first zinc(++) metallo enzyme found in 1940, is one 29.3-kDa protein with 260 amino residues. It is the most efficient isoenzyme for CO₂ hydration with k_{cat} of about

$1.6 \times 10^6 \text{ s}^{-1}$ at 25 °C and pH 9 [1]. The active sites of hCAII are located at a large cone-shaped cavity containing a catalytic Zn²⁺ unit lying at the bottom of the cavity, where it is coordinated in a tetrahedral geometry by the imidazole side chains of His94, His96, His119 and one H₂O or OH⁻. In addition, one hydrophobic pocket cooperating with CO₂ near the tetrahedral geometry is formed by Val121, Val143, Leu198, and Trp209 [2–4]. hCAII has a wide distribution and is found in many different organs and cell types. It is involved in many crucial physiologic and pathologic processes, such as bone resorption, calcification, glaucoma and tumorigenesis [1,2]. Thus it has become an important target for potential drug design and clinical applications. Two classes of carbonic anhydrase inhibitors (CAIs) are known: monovalent anions and sulfonamides (RSO_2NH_2 or RSO_2NHOH), the latter are the most important CAIs [5]. Many sulfonamide inhibitors are designed and

* Corresponding author. Tel./fax: +86 871 5223800.

E-mail address: nhtan@mail.kib.ac.cn (N. Tan).

synthesized since the first sulfonamide was discovered 66 years ago [6], some of which have been clinically used as antiglaucoma or antiepilepsy agents for decades, such as dorzolamide (DZA), methazolamide (MZA), dichlorophenamide (DCP) [5].

Experimental research about CAII has been run in our lab for several years. Preliminary studies showed that some natural products appeared to have potential inhibitory activities against CAII [2,7]. Obviously, the interaction mechanism of CAII and its inhibitors would be greatly helpful in discovering its novel natural inhibitors. Recently, Supuran and co-workers have reported a new series of sulfonamides incorporating 1,3,5-triazine and some acetazolamide derivatives which showed potent human carbonic anhydrase II inhibitory activities with K_i values [8–10]. In this study, 3D-QSAR models were developed based on these sulfonamide inhibitors. With the methods of Comparative of Molecular Field Analysis (CoMFA) and Comparative of Molecular Similarity Indices Analysis (CoMSIA), it is possible to further understand structural features of CAII and to find out the interactions between the structural information of these sulfonamide inhibitors and their potential activities. And it can also provide quantitative estimation of activity and insights into key structural elements to design new CAII potential lead candidates.

2. Experimental methods

2.1. Data set and molecular modeling

A series of 61 potent aromatic and heterocyclic sulfonamide derivatives [8–10] were performed in this study (Table 1). In vitro CAII inhibitory activities were converted into the corresponding pK_i ($-\log K_i$) values. The total set of CAII inhibitors (61 compounds) was randomly divided into the training set (51 compounds) and test set (10 compounds, labeled with an asterisk).

The three-dimensional structures of sulfonamide derivatives were constructed by using Sybyl program package version 6.9 [11] on a Silicon Graphic workstation. Energy minimizations were performed using the Tripos force field [12] and the Gasteiger–Huckel charge with a distance-dependent dielectric and conjugate gradient method. The convergence criterion was 0.01 kcal/mol Å.

2.2. Alignment

The most important requirement for CoMFA and CoMSIA studies is that the 3D structures were aligned according to a suitable conformational template, which is assumed to be one ‘bioactive’ conformation [13]. In this study, two alignment methods were carried out. In receptor-based model the molecules were aligned according to the bioactive conformations obtained from docking. The FlexX program (Tripos, St. Louis, MO), which was successfully used previously in our lab [14], was used to dock all compounds into the active sites of CAII, and for each ligand 30 conformations were obtained. The conformation with the best Total Score was

selected as the most probable binding conformation (bioactive conformation). These bioactive conformations were aligned together inside the active sites and used for CoMFA and CoMSIA analyses. In ligand-based model the crystal structure of the ligand (SFB555, Fig. 1) from the complex of CAII (PDB ID: 1GID) was used as template structure for the alignment and $H_2NSO_2^-$ (red color) was used as common fragment. Compounds of the training set were aligned on template by using “align database” option given in Sybyl. Fig. 1 shows SFB555 structure and alignment structures in the training set.

2.3. CoMFA

Steric and electrostatic interactions were calculated using an sp^3 carbon atom and a +1 charge as steric and electrostatic probes, respectively, with Tripos force field. The CoMFA grid spacing was 2.0 Å in the x , y and z directions. The default value of 30 kcal/mol was set as the maximum steric and electrostatic energy cutoff. Minimum-sigma (column filtering) was set to be 2.0 kcal/mol. The CoMFA method was also used successfully in our lab previously in the 3D-QSAR studies of aldehyde inhibitors of human cathepsin K [15].

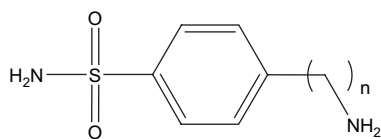
2.4. CoMSIA

The CoMSIA method defines five fields: steric, electrostatic, hydrophobic, H-bond donor and H-bond acceptor, which were calculated at each lattice interactions of a regularly spaced grid of 2.0 Å. A probe atom with radius 1.0 Å, +1 charge, hydrophobicity +1.0, and H-bond donor and acceptor properties of +1.0 was used to calculate steric, electrostatic, hydrophobic, and H-bond donor and acceptor fields. A distance-dependent Gaussian type functional form will be taken into account abrupt changes of potential energy near the molecular surface. The default value of 0.3 was used as the attenuation factor.

2.5. Partial least square (PLS) analysis

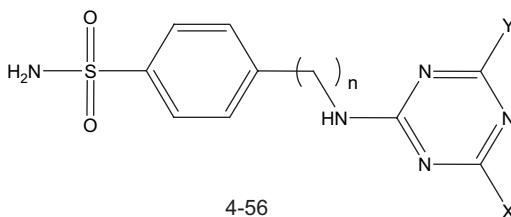
The CoMFA and CoMSIA descriptors were used as independent variables, and pK_i values as dependent variables in partial least square regression analysis. Cross-validation partial least square method of leave-one-out (LOO) was performed to obtain the optimal number of components used in the subsequent analysis. The minimum-sigma (column filtering) was set to be 2.0 kcal/mol (CoMFA) and 1.0 kcal/mol (CoMSIA) to improve the signal-to-noise ratio. The optimum number of principle components in the final non-cross-validated QSAR equations was determined to be that leading to the highest correlation coefficient (r^2) and the lowest standard error in the LOO cross-validated predictions. The non-cross-validation was used in the analysis of CoMFA and CoMSIA results and the prediction of the models.

Table 1

Structures, experimental and predicted pK_i , residuals by CoMFA and CoMSIA models in the training set and test set (with *) with receptor-based method

1-3

Comp.	<i>n</i>	pK_i Exp.	Receptor-based model			
			CoMFA		CoMSIA	
			Predicted.	Residual.	Predicted.	Residual.
1	0	6.52	6.56	−0.04	6.46	0.06
2	1	6.77	6.88	−0.11	6.77	0.00
3	2	6.80	6.91	−0.11	6.76	0.04



4-56

Comp.	X, Y	<i>n</i>	pK_i Exp.	Receptor-based model			
				CoMFA		CoMSIA	
				Predicted.	Residual.	Predicted.	Residual.
4	Cl, Cl	0	6.97	7.02	−0.05	6.95	0.02
5	Cl, Cl	1	7.89	6.98	0.91	7.92	−0.03
6	Cl, Cl	2	7.68	7.73	−0.05	7.71	−0.03
7	OH, OH	0	6.56	6.49	0.07	6.58	−0.02
8	OH, OH	1	6.89	6.93	−0.01	6.91	−0.02
9	OH, OH	2	7.01	7.09	−0.08	7.01	0.00
10	NHMe, NHMe	0	7.64	7.61	0.03	7.69	−0.05
11	NHMe, NHMe	1	7.82	7.71	0.11	7.71	0.11
12*	NHMe, NHMe	2	7.57	7.77	−0.20	7.72	−0.25
13	OMe, OMe	0	7.44	7.47	−0.03	7.47	−0.30
14	OMe, OMe	1	6.95	7.38	−0.43	7.16	−0.21
15	OMe, OMe	2	7.68	7.72	−0.04	7.69	−0.01
16	OEt, OEt	0	7.70	7.61	0.09	7.48	0.22
17	OEt, OEt	1	7.08	7.18	−0.10	6.99	0.09
18*	OEt, OEt	2	7.64	7.31	0.33	7.35	0.29
19*	OPh, OPh	0	6.86	7.11	−0.25	6.57	0.29
20	OPh, OPh	1	6.91	6.99	−0.08	6.97	−0.06
21	OPh, OPh	2	7.08	7.05	0.03	7.16	−0.08
22*	NH ₂ , NH ₂	1	7.80	6.96	0.84	7.55	0.25
23	NH ₂ , NH ₂	2	7.68	7.60	0.08	7.71	−0.03
24	NHNH ₂ , NHNH ₂	0	7.74	7.72	0.02	7.76	−0.02
25	NHNH ₂ , NHNH ₂	1	7.57	7.51	0.06	7.60	−0.03
26	NHNH ₂ , NHNH ₂	2	7.51	7.54	−0.03	7.47	0.04
27	NHEt, NHEt	1	7.85	7.72	0.13	7.73	0.12
28	NHEt, NHEt	2	7.64	7.46	0.18	7.55	0.09
29*	<i>i</i> -PrHN, <i>i</i> -PrHN	0	7.42	7.53	−0.11	7.43	−0.01
30	<i>i</i> -PrHN, <i>i</i> -PrHN	1	7.34	7.51	−0.17	7.50	−0.16
31	<i>i</i> -PrHN, <i>i</i> -PrHN	2	7.30	7.35	−0.05	7.35	−0.05
32	<i>n</i> -PrHN, <i>n</i> -PrHN	0	7.31	7.35	−0.04	7.24	0.07
33	<i>n</i> -PrHN, <i>n</i> -PrHN	1	7.20	7.18	0.02	7.11	0.09
34	<i>n</i> -PrHN, <i>n</i> -PrHN	2	7.08	7.21	−0.13	7.17	−0.09
35*	<i>n</i> -BuHN, <i>n</i> -BuHN	0	6.84	7.37	−0.53	7.19	−0.35
36	<i>n</i> -BuHN, <i>n</i> -BuHN	1	6.76	6.75	0.01	6.80	−0.04

(continued on next page)

Table 1 (continued)

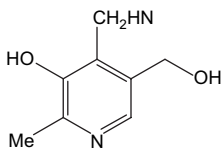
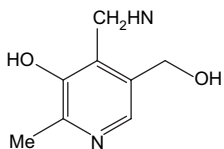
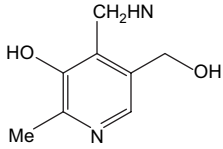
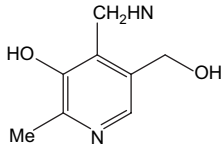
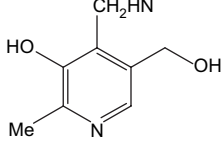
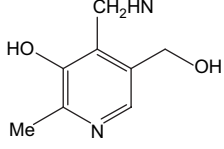
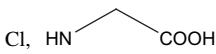
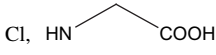
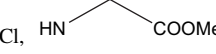
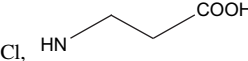
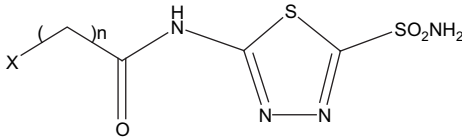
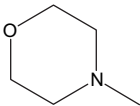
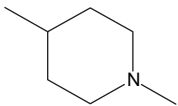
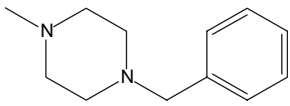
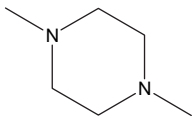
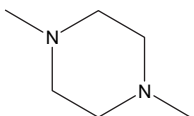
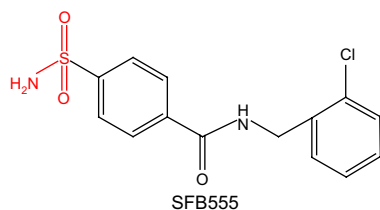
Comp.	X, Y	<i>n</i>	pK_i				
			Exp.	Receptor-based model			
				CoMFA		CoMSIA	
				Predicted.	Residual.	Predicted.	Residual.
37	<i>n</i> -BuHN, <i>n</i> -BuHN	2	6.79	6.69	0.10	6.78	0.01
38	Et ₂ NCH ₂ CH ₂ HN, Et ₂ NCH ₂ CH ₂ HN	0	6.67	6.59	0.08	6.63	0.04
39	[HN(CH ₂ CH ₂) ₂ N]CH ₂ CH ₂ HN, [HN(CH ₂ CH ₂) ₂ N]CH ₂ CH ₂ HN	0	6.49	6.51	−0.02	6.46	0.03
40	[HN(CH ₂ CH ₂) ₂ N]CH ₂ CH ₂ HN, [HN(CH ₂ CH ₂) ₂ N]CH ₂ CH ₂ HN	1	6.47	6.47	0.00	6.49	−0.02
41	 , 	0	6.34	6.29	0.05	6.32	0.02
42	 , 	1	6.22	6.19	0.03	6.23	−0.01
43*	 , 	2	6.12	6.67	−0.55	6.77	−0.65
44*	NMe ₂ , NMe ₂	0	7.41	7.53	−0.12	7.35	0.06
45	NMe ₂ , NMe ₂	1	7.48	7.65	−0.17	7.61	−0.13
46	NMe ₂ , NMe ₂	2	7.46	7.43	0.03	7.41	0.05
47	NEt ₂ , NEt ₂	0	7.49	7.25	0.24	7.25	0.24
48	NEt ₂ , NEt ₂	1	7.21	7.23	−0.02	7.23	−0.02
49	NEt ₂ , NEt ₂	2	7.11	7.01	0.10	7.17	−0.06
50	NMe ₂ , <i>Nn</i> -Pr ₂	0	7.41	7.41	0.00	7.40	0.01
51	NMe ₂ , <i>Nn</i> -Pr ₂	1	7.48	7.45	0.03	7.38	0.10
52*	NMe ₂ , <i>Nn</i> -Pr ₂	2	7.44	7.38	0.06	7.15	0.29
53	Cl, 	1	7.54	7.52	0.02	7.59	−0.05
54	Cl, 	2	7.49	7.43	0.06	7.46	0.03
55*	Cl, 	2	7.48	7.47	0.01	7.41	0.07
56	Cl, 	2	7.55	7.53	0.02	7.54	0.01

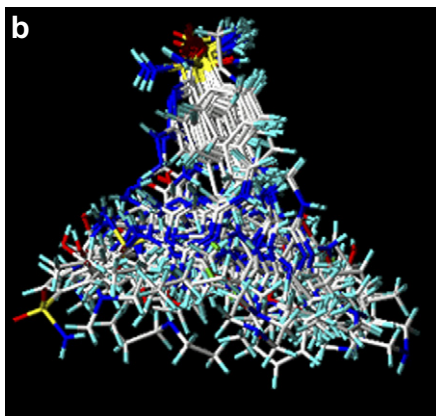
Table 1 (continued)

<div style="text-align: center;">  <p>57-61</p> </div>							
Comp.	X	n	p <i>K_i</i> Exp.	Receptor-based model			
				CoMFA		CoMSIA	
				Predicted.	Residual.	Predicted.	Residual.
57		1	9.05	9.05	0.00	9.02	0.03
58		1	8.42	8.45	−0.03	8.45	−0.03
59		1	8.74	8.77	−0.03	8.71	0.06
60		1	8.80	8.78	0.02	8.77	0.03
61		2	8.72	8.68	0.04	8.75	−0.03

a



b



c

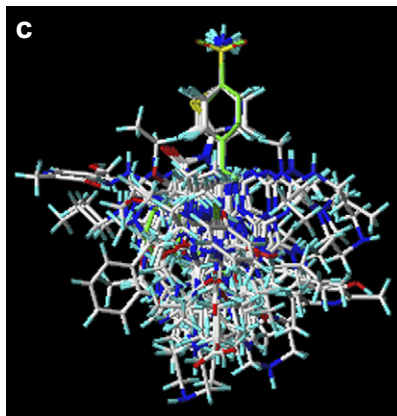


Fig. 1. Alignment of the training set: a is the template structure (common fragment in red), b is the alignment of the training set for receptor-based model and c is the alignment on the template (green) for ligand-based model.

Table 2
Summary of CoMFA and CoMSIA model results

Component	Receptor-based model		Ligand-based model	
	CoMFA	CoMSIA	CoMFA	CoMSIA
q^2	0.623	0.562	0.532	0.466
r^2	0.986	0.987	0.962	0.961
n	6	8	5	5
F value	498.1	392.0	225.3	220.4
SEE	0.080	0.079	0.130	0.131
Steric	0.464	0.143	0.434	0.160
Electrostatic	0.536	0.258	0.566	0.258
Hydrophilic	—	0.223	—	0.234
Donor	—	0.251	—	0.150
Acceptor	—	0.125	—	0.198

q^2 , LOO cross-validated correlation coefficient; r^2 , non-cross-validated correlation coefficient; n , number of components used in the PLS analysis; SEE, standard error of estimate; F value, F -statistic for the analysis.

3. Results and discussion

The CoMFA and CoMSIA field analyses were generated for both the ligand-based model and receptor-based model. The receptor-based model gave the cross-validated coefficient q^2 values of 0.623 and 0.562 for CoMFA and CoMSIA (Table 2), respectively, which were much better than those of the ligand-based model giving the q^2 values of 0.532 and 0.466. Hence the receptor-based model was taken up for further consideration. Table 1 lists experimental activities, predicted activities and residual values of the training set and test set by CoMFA and CoMSIA models.

3.1. CoMFA model (receptor-based model)

CoMFA analysis was performed based on the alignment of bioactive conformations obtained from the docking of 51 compounds in the training set. PLS analysis yielded a cross-validated correlation coefficient q^2 of 0.566. Activity of compound 5 in the training set is poorly predicted with residuals 0.91 by this model. Performing PLS analysis omitting compound 5 yielded q^2 value of 0.623, which gave a better result. The non-cross-validated PLS analysis gave a correlation

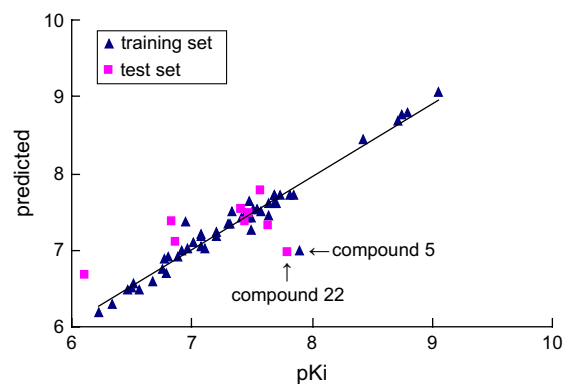


Fig. 2. Experimental activities versus predicted activities for compounds in the training and test sets using CoMFA model.

coefficient r^2 of 0.986 with an SEE of 0.080. The steric and electrostatic contributions are 0.464 and 0.536. Fig. 2 shows correlation between the experimental activities and predicted ones in the training and test sets by this CoMFA model.

The CoMFA contour plots of steric and electrostatic interactions are shown in Fig. 3. In Fig. 3a, one big green contour around the 1,3,5-triazole ring indicates that steric bulk is favored for activity in these areas. This can be explained by the fact that it shows stronger activity when one hydrogen atom of amido is substituted by the 1,3,5-triazole ring. For example, compounds 10, 13, 16, 44, and 47 are more active than compounds 1, 2 and 3. There are one big yellow contour and two medium yellow contours (one is behind the green contour) away from the 4- and 6-position of the 1,3,5-triazole ring, which indicate that steric bulk is disfavored for activity in these areas. For example, the inhibitory activity of compounds 27, 33, 36, 40 and 42 is ordered as 27 > 33 > 36 > 40 > 42. Moreover, as the number of methylene (n) increased from 0 to 2, activity of some compounds decreased such as 32 > 33 > 34, 41 > 42 > 43 and 47 > 48 > 49.

In Fig. 3b, there is one big blue contour around the 4- or 6-position of the 1,3,5-triazole ring, which indicates that any positive charge is favored for activity in these areas. This can be explained by the fact that compounds 22 and 23 are strongly active than compounds 8 and 9. One medium blue

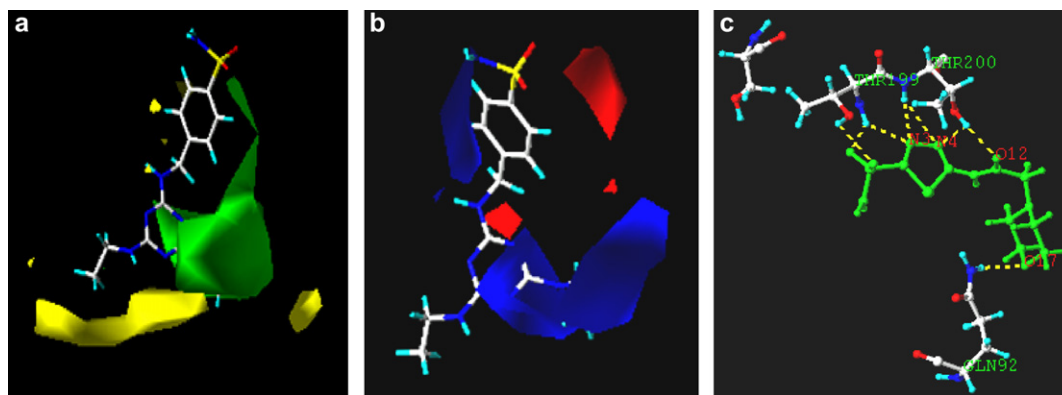


Fig. 3. CoMFA contour maps in combination with compound 27: (a) the steric field distribution; (b) the electrostatic distribution. Sterically favored areas in green; sterically disfavored areas in yellow. Positive potential favored areas in blue; negative potential favored areas in red. (c) H-bond interactions of compound 27 (green) with active sites of CAII.

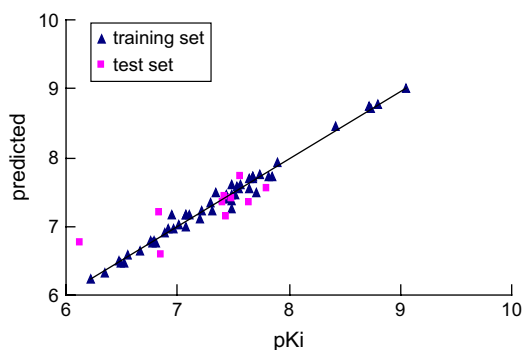


Fig. 4. Experimental activities verse predicted activities for compounds in the training and test sets using CoMSIA model.

contour near the benzene ring seems to be contradictory with the red contour which is away from the benzene ring. This may explain that when $n = 2$ the substituting groups in 4- or 6-position of the 1,3,5-triazole ring can superpose with the benzene ring. One small red contour above 1,3,5-triazole ring indicates that negative charge group is favored for activity in these areas. The fact that one hydrogen substituted by the triazole ring greatly increases the activity can explain it. The red contour away from benzene ring indicates that any negative charge group is favored for activities in these areas. According to the receptor-based alignment, the 1,3,4-thiadiazole ring of compounds **57–61** was in the same areas of benzene ring. Then the fact that heterocyclic sulfonamides (**57–61**) are more active than benzene sulfonamides may interpret the red contour away from benzene ring. Performing a particular study of compounds **57–61** showed that the atoms N3 and N4 of 1,3,4-thiadiazole ring can form four H-bond interacting with Thr199 and Thr200 and O12 have H-bond interaction with Thr200 (Fig. 3c).

3.2. CoMSIA model (receptor-based model)

CoMSIA analysis was performed using the following descriptor fields: steric, electrostatic, hydrophilicity, H-bond donor and H-bond acceptor. The CoMSIA results are summarized in Table 2. A cross-validated correlation coefficient q^2 of

0.562 and a non-cross-validated correlation coefficient r^2 of 0.987 with SEE of 0.079 were obtained when all the five descriptors were considered. These results indicate that a reliable CoMSIA model was successfully constructed. Fig. 4 shows the experimental activities versus predicted ones in the training and test sets by this CoMSIA model.

Fig. 5a and b shows the steric and electrostatic contour maps of the CoMSIA model, which are similar to the CoMFA model maps in Fig. 3a and b.

Fig. 5c described an overlay of the hydrophobic CoMSIA field with the active sites of CAII. Two yellow hydrophobic favored contours corresponding to the benzene ring and methylene group are satisfied by Leu198 and Phe131. There is one big white hydrophilic favored contour around the 1,3,5-triazole ring, which is partly surrounded by a hydrophilic pocket formed by His64, Thr200 and Pro201 and partly exposed in solvent.

Fig. 6a depicts an overlay of H-bond donor field distribution of CoMSIA model with the active sites of CAII. One big cyan contour near the sulfanilamide $-NH_2$ indicates that proton acceptors are expected in the receptor, which can be interpreted by the H-bond acceptor of His94 and His119.

Fig. 6b depicts an overlay of H-bond acceptor field distribution of CoMSIA model with the active sites of CAII. One big H-bond acceptor magenta contour near the sulphonyl indicates that proton donors are favored for activity in these areas in the receptor, which is satisfied by the proton donor of Thr199 and Thr200.

3.3. Outliers

In CoMFA model there were two outliers of compounds **5** and **22** with the residuals of 0.91 and 0.84, respectively. The substituting groups of **5** and **22** are Cl and NH_2 , respectively, which are both hydrophilic and are H-bond acceptor or donor. They may have hydrophobic and H-bond interactions with amino residues of CAII and these interactions may be important to their activities. However, comparing CoMFA and CoMSIA methods, CoMFA analysis does not consider hydrophobic and H-bond fields. So activities of **5** and **22** may not be predicted exactly by CoMFA model but could be predicted well

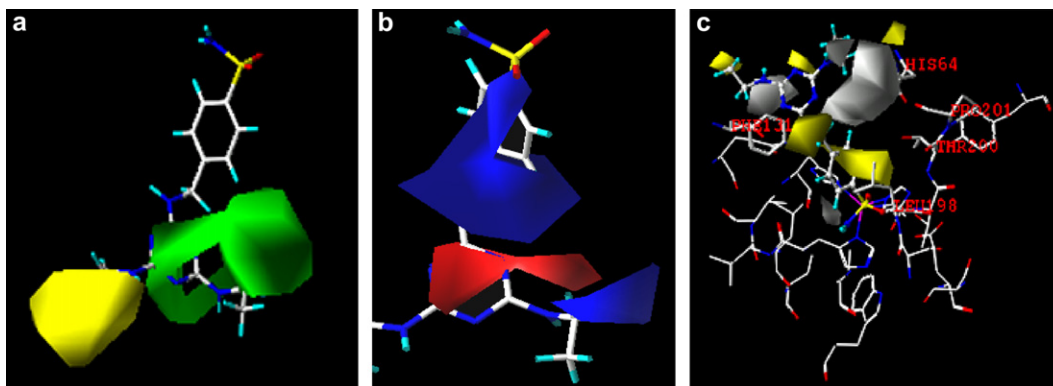


Fig. 5. CoMSIA contour maps in combination with compound **27**: (a) the steric field distribution; (b) the electrostatic field distribution; (c) the hydrophobic field distribution projected in the active sites. Sterically favored areas in green; sterically disfavored areas in yellow. Positive potential favored areas in blue; negative potential favored areas in red. Hydrophobic favored areas in yellow; hydrophilic favored areas in white.

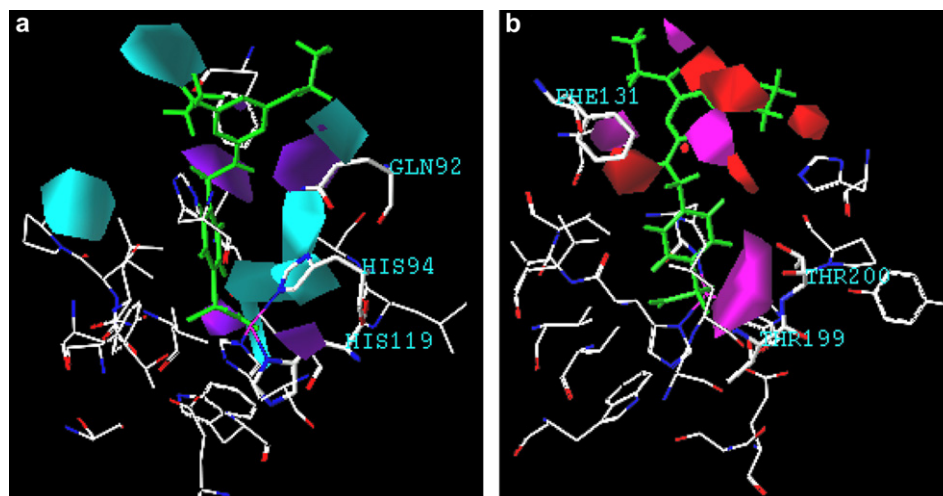


Fig. 6. CoMSIA contour maps in combination with compound **27** (green) projected in the active sites: (a) CoMSIA H-bond donor field distribution; (b) CoMSIA H-bond acceptor field distribution. H-bond donor favored areas in cyan; H-bond donor disfavored areas in purple. H-bond acceptor favored areas in magenta; H-bond acceptor disfavored areas in red.

by CoMSIA model (residuals of -0.03 and 0.25 for **5** and **22**, respectively). Those may be the reason that compounds **5** and **22** were poorly predicted by CoMFA model.

3.4. Validation

Ten randomly selected compounds were used as the test set to verify the constructed CoMFA and CoMSIA models. Calculated results were listed in Table 1 and displayed in Figs. 2 and 4. The predicted pK_i with these 3Q-QSAR models are in good agreement with the experimental data within a statistically tolerable error range, with a correlation coefficient of $r^2 = 0.35$ and 0.62 for CoMFA and CoMSIA models, respectively. In CoMFA model, compound **22** is poorly predicted (residuals $= 0.86$), but the r^2 value rose to 0.74 omitting compound **22**. Testing results indicate that the CoMFA and CoMSIA models could be reliably used in novel inhibitors design for developing drug leads against CAII.

4. Conclusion

The ligand-based and receptor-based 3D-QSAR analyses of 61 sulfonamide inhibitors of CAII were carried out using CoMFA and CoMSIA models. Comparing these two methods, the receptor-based model gave q^2 and r^2 values for CoMFA and CoMSIA of 0.623 and 0.986 , 0.562 and 0.987 , respectively, which were much better than those of the ligand-based model. The consistency between CoMFA and CoMSIA field distributions shows the robustness of these 3D-QSAR models. Results of CoMFA and CoMSIA field analysis suggested that heterocyclic sulfonamide inhibitors of CAII are more active than aromatic sulfonamide inhibitors, in the latter 1,3,5-triazole group substituting one hydrogen atom of the amido is favored and the moderate groups in its 4- and 6-position are required. Thus, the information obtained from this study can be utilized to further develop novel inhibitors of CAII.

Acknowledgments

The present work was supported by the Foundation of Chinese Academy Sciences (West Light Program, KSCX1-09-03-1 and KSCX-SW-11) and the National Natural Science Foundation of China (30572258).

References

- [1] G.Z. Zeng, H.Q. Huang, N.H. Tan, C.J. Ji, X.L. Pan, *Acta Bot. Yunnan.* 28 (2006) 543–552.
- [2] N.H. Tan, X. Fu, C.J. Ji, G.Z. Zeng, L.H. Jiang, R.R. Jia, *Chin. J. Org. Chem.* 24 (Suppl. 139) (2004).
- [3] J.E. Jackman, K.M. Merz Jr., C.A. Fierke, *Biochemistry* 35 (1996) 16421–16428.
- [4] N. Vicker, Y. Ho, J. Robinson, L.L.W. Woo, A. Purohit, M.J. Reed, B.V.L. Potter, *Bioorg. Med. Chem. Lett.* 13 (2003) 863–865.
- [5] C.T. Supuran, A. Scozzafava, A. Casini, *Med. Res. Rev.* 23 (2003) 146–189.
- [6] T.H. Maren, C.W. Conroy, *J. Biol. Chem.* 268 (1993) 26233–26239.
- [7] X. Fu, N.H. Tan, L.H. Jiang, R.R. Jia, C.J. Ji, J. Landro, A. Fekete, H. Mueller, T. Henkel, *Acta Bot. Yunnan* 25 (2003) 724–729.
- [8] V. Garaj, L. Puccetti, G. Fasolis, J.-Y. Winum, J.-L. Montero, A. Scozzafava, D. Vullo, A. Innocenti, C.T. Supuran, *Bioorg. Med. Chem. Lett.* 15 (2005) 3102–3108.
- [9] H. Turkmen, M. Durgun, S. Yilmaztekin, M. Emul, A. Innocenti, D. Vullo, A. Scozzafava, C.T. Supuran, *Bioorg. Med. Chem. Lett.* 15 (2005) 367–372.
- [10] V. Garaj, L. Puccetti, G. Fasolis, J.-Y. Winum, J.-L. Montero, A. Scozzafava, D. Vullo, A. Innocenti, C.T. Supuran, *Bioorg. Med. Chem. Lett.* 14 (2004) 5427–5433.
- [11] Sybyl Version 6.9, Tripos Associates, St. Louis (MO), 2001.
- [12] M. Clark, R.D. Cramer, N.V. Opdenbosch, *J. Comput. Chem.* 10 (1989) 982–1012.
- [13] H. Parra-Delgado, C.M. Compadre, T. Ramírez-Apan, M.J. Muñoz-Fam-buena, R.L. Compadre, P. Ostrosky-Wegman, M. Martínez-Vázquez, *Bioorg. Med. Chem.* 14 (2006) 1889–1901.
- [14] X.L. Pan, N.H. Tan, G.Z. Zeng, Y.M. Zhang, R.R. Jia, *Bioorg. Med. Chem.* 13 (2005) 5819–5825.
- [15] X.L. Pan, N.H. Tan, G.Z. Zeng, H.J. Han, H.Q. Huang, *Bioorg. Med. Chem.* 14 (2006) 2771–2778.